Applied Thermal Engineering 62 (2014) 671–679

Contents lists available at ScienceDirect

Applied Thermal Engineering

journal homepage: www.elsevier.com/locate/apthermeng

Theoretical investigation of stable dropwise condensation heat transfer on a horizontal tube

H.W. Hu, G.H. Tang*

MOE Key Laboratory of Thermo-Fluid Science and Engineering, School of Energy and Power Engineering, Xi'an Jiaotong University, Xi'an 710049, PR China

ARTICLE INFO

Article history:
Received 10 September 2013
Accepted 14 October 2013
Available online 23 October 2013

Keywords:
Theoretical model
Dropwise condensation heat transfer
Contact angle
Horizontal tube

ABSTRACT

The heat transfer model of stable dropwise condensation for saturated vapor on a horizontal tube is developed based on previous theoretical models. Through a comprehensive analysis of all the contributing thermal resistances, the convection effect inside the droplet itself is taken into consideration in the model. For the stable dropwise condensation process in dynamic conservation, a method of double integration of heat flux through numerous inclined plates with different inclination angles is introduced to obtain the overall heat flux through the horizontal tube surface. The model can predict the variation of heat transfer of stable dropwise condensation with different contact angles outside a horizontal tube. The influences of contact angle, temperature difference, and other typical parameters on both a single droplet and the whole condensation process are discussed. The results indicate that a high contact angle can cause a size reduction of falling droplets from condensing surface and thus taking more heat away. The adsorbed condensate film adds an extra thermal resistance and its thickness plays a significant role on the dropwise condensation heat transfer.

1. Introduction

Condensation heat transfer is an important and ubiquitous process in many fields, which has been widely applied in various industries such as in the power generation industry, residual heat and water recovery engineering and desalination process. According to the wetability of condensate on the cool surface, the condensation process can be divided into two types: film condensation and dropwise condensation. For the theoretical research of film condensation, Nusselt [1] first proposed a theoretical analytical solution for the pure vapor on a vertical plate. Subsequently, theoretical analysis for film condensation had been expanded and developed extensively in more complex environments. Recently, the condensation technology on the microchannel surface is developed to obtain higher heat transfer efficiency in the limited space, and a lot of theoretical researches have also been carried out for the film condensation on the microchannel surface [2–5]. Nevertheless, as we know, compared with film condensation, the dropwise condensation exhibits much higher heat transfer performance, which has also attracted considerable attention.

Scholars began to study the formation mechanism of dropwise condensation from the beginning of the last century. Jakob et al. [6] first proposed the thin film fracture condensation mechanism. It is suggested that a thin condensate film could be firstly formed on the condensing surface as the steam comes into contact with the condensing surface, and then the thin film thickens gradually with the increase of the condensate. At this stage the latent heat of condensation can only be transmitted through the thin film. Rupture will occur until the thickness of the film reaches a critical value, and then small droplets can appear due to the effect of surface tension. This formation mechanism has been verified experimentally and developed further by Ruckenstein and other scholars [7].

Subsequently, some researchers [8–11] put forward and verified the nucleation condensation mechanism for dropwise condensation formation, which is distinct from the thin film fracture condensation mode. It is indicated that dropwise condensation is a nucleation phenomenon, analogous to the nucleate boiling. The vapor has priority to condensate into small droplets on the nucleation sites due to the high surface free energy and with the growth of small droplets, and their position centers are not confined to the nucleation sites, especially at the stage of merger and shedding. Over the years, most experimental and theoretical studies of dropwise condensation have been conducted based on the certain nucleation condensation formation mechanism.

* Corresponding author. Tel.: +86 29 82665319; fax: +86 29 82665445.
E-mail address: ghtang@mail.xjtu.edu.cn (G.H. Tang).

1359-4311/$ – see front matter © 2013 Elsevier Ltd. All rights reserved.
http://dx.doi.org/10.1016/j.applthermaleng.2013.10.022

Nomenclature

d_c	contact diameter of droplet (m)
$f(\theta, \alpha)$	shape factor function
F_c	surface tension force (N)
F_g	gravity force (N)
h_{av}	average heat transfer coefficient (W/(m^2 K))
h_{film}	heat transfer coefficient through condensate film (W/(m^2 K))
h_i	interfacial heat transfer coefficient (W/(m^2 K))
H_{fg}	latent heat of vaporization (J/kg)
g	gravitational acceleration (m/s^2)
M	relative molecular mass
n	population density of small drops (m^{-3})
N	population density of large drops (m^{-3})
P	vapor pressure (Pa)
r	droplet radius (m)
r_e	effective droplet radius (m)
r_{max}	maximum droplet radius (m)
r_{min}	minimum droplet radius (m)
R	universal gas constant (J/(mol K))
R_c	thermal resistance due to droplet curvature (K)
R_{coat}	thermal resistance through the coating layer (m^2 K/W)
R_d	conduction resistance through droplet (m^2 K/W)
R_{film}	thermal resistance through condensate film (m^2 K/W)
R_i	vapor–liquid interfacial resistance (m^2 K/W)
T_s	vapor saturation temperature (K)
ΔT	surface subcooling temperature (K)
ΔT_c	temperature difference due to drop curvature (K)
ΔT_d	temperature difference due to conduction through droplet (K)
ΔT_i	temperature difference due to interfacial resistance (K)
s	arc length (m)
q	dropwise condensation heat flux (W/(m^2 K))
V	specific volume of vapor (m^3/kg)

Greek symbols

α	inclination angle (deg)
α_c	condensation coefficient
θ	contact angle (deg)
θ'	local contact angle (deg)
θ_a	advancing contact angle (deg)
θ_r	receding contact angle (deg)
η	area ratio
ρ	density of liquid (kg/m^3)
λ_{coat}	thermal conductivity of coating material (W/(m K))
λ	thermal conductivity of liquid (W/(m K))
δ	thickness of condensate film (m)
δ_{coat}	thickness of coating layer (m)
σ_{lv}	surface tension (N/m)
Φ	heat transfer rate (W)
ϕ_1	contact area between small droplet and condensing surface (m^2)
ϕ_2	contact area between large droplet and condensing surface (m^2)

Recently, droplets and film coexisting condensation mechanism based on the adsorption theory was proposed by Song et al. [12]. They observed the initial droplet formation process by using reflectance spectroscopy and it is indicated that not only several droplet nucleation sites but also the adsorbed condensate film existed on the condensing surface, which has been more and more validated by testing with high-tech instruments and advanced experiments [13,14].

Simultaneously, a lot of experimental and numerical researches have also been conducted and developed in terms of superior heat transfer performance and sustainability of dropwise condensation. Rausch et al. [15] achieved stable dropwise condensation of steam near atmospheric pressure by ion beam implantation of N^+ on titanium surfaces, and they indicated that the nucleation mechanism was possibly caused by interactions of nanoscale surface roughness and surface chemistry effects connected with precipitation of nitrides. Walpot et al. [16] experimentally investigated the thermal efficiency in compact heat exchangers using epoxy coatings with good adhesion characteristics. Bansal et al. [17] achieved the clear dropwise condensation of water on a horizontally placed transparent polymer substrate, and they attempted to experimentally determine the heat transfer coefficient driven by a small temperature difference. The organic self-assembled-monolayer and polytetrafluoroethylene (PTFE) coatings [18–20] were used to enhance steam condensation through dropwise condensation. In addition, with the fractal theory applied in porous media [21], the random fractal model was employed to simulate the droplet spatial distribution and heat transfer in dropwise condensation in the literature [22–24].

Although a large number of theoretical and experimental studies on the mechanism and characteristics of dropwise condensation heat transfer have been carried out, the research mostly concentrates on dropwise condensation heat transfer without considering the convection effect inside the droplets and the geometries are mostly limited to the plate or vertical wall. The theoretical investigation of the stable dropwise condensation on a horizontal tube is rarely seen in the literature. The current study presents a dropwise condensation heat transfer model including the variation of the drop-size distribution based on the droplets and film coexisting condensation mechanism on the horizontal tube. On the analysis of all the contributing thermal resistances, the convection effect inside the droplets themselves is taken into account. The rest of the paper is organized as follows. In Section 2, we present the modeling process for dropwise condensation heat transfer on the horizontal tube. In Section 3, the theoretical predictions of dropwise condensation heat transfer performance are presented, and influences of contact angle, subcooling, and other typical parameters on the heat transfer characteristics of both the single droplet and stable dropwise condensation process are also discussed. Finally, a brief conclusion is given in Section 4.

2. Heat transfer model

Based on the droplets and film coexisting condensation mechanism, the heat transfer resistance in dropwise condensation process between the vapor and condensing surface can be divided into two independent parts: one is the heat transfer resistance through droplets of all sizes and the other is that through the adsorbed condensate film (Fig 1). Above all, we neglect some secondary factors in the theoretical analysis and the following assumptions are made:

(1) The contact angle on the condensing surface is fixed regardless of the drop size and the temperature of vapor and condensing surface.
(2) Thermal properties of the condensate are evaluated at the temperature $(T_v + T_w)/2$.

(3) The shape of droplets is a section of a sphere, and the effect of shape change on condensation process is neglected.
(4) The droplet size is very small compared to the diameter of the horizontal tube. In other words, the curvature of the coverage area at the bottom of droplets is negligible.
(5) The drop-size distribution of all sized droplets is steady, and the nucleation sites are random on the condensing surface.
(6) Non-uniform distribution of the heat flux through the independent parts is neglected. And the non-uniform distribution of condensing surface temperature caused by the drop-size distribution and the low thermal conductivity of coating layer is neglected as well, i.e., the constriction resistance on the condensing surface is not considered.

2.1. Heat transfer through the adsorbed condensate film

The thermal resistance through the adsorbed condensate film is composed of vapor–liquid interfacial resistance, conduction resistance through condensate film and conduction resistance through coating layer. In the present model, vapor–liquid interface is assumed to be smooth and non-wavy and the thickness of condensate film is uniform by ignoring the effect of gravity in the steady state. Therefore, the thermal resistance through the adsorbed condensate film can be expressed as

$$R_{\text{film}} = \frac{1}{h_{\text{film}}} = \frac{1}{h_{\text{i}}} + \frac{\delta}{\lambda} + \frac{\delta_{\text{coat}}}{\lambda_{\text{coat}}} \tag{1}$$

where δ and δ_{coat} are the thickness of the condensate film and coating material, respectively, and similarly, λ and λ_{coat} are the thermal conductivity of the condensate film and coating material, respectively. And h_{i} is the interfacial heat transfer coefficient, which can be written as [25]

$$h_{\text{i}} = \frac{2\alpha_{\text{c}}}{2-\alpha_{\text{c}}}\left(\frac{M}{2\pi R T_{\text{s}}}\right)^{\frac{1}{2}}\frac{H_{\text{fg}}^2}{T_{\text{s}}V} \tag{2}$$

where H_{fg}, T_{s}, V and M are the latent heat of vaporization, saturation temperature, specific volume, and relative molecular mass of the vapor, respectively. And α_{c} is defined as the condensation coefficient, which can be taken as unity when the steam contains no non-condensable gas.

2.2. Heat transfer through a single condensing droplet

In the process of stable dropwise condensation, each droplet contributes to the condensation by transferring heat through itself. Therefore, evaluating the heat transfer through a single condensing droplet and analyzing the influence of various factors are highly necessary for predicting the overall heat transfer behavior of dropwise condensation.

Firstly, the heat released by vapor transfers through the vapor–liquid interface, and the vapor–liquid interfacial resistance is expressed as the temperature difference

$$\Delta T_{\text{i}} = \frac{\Phi}{2\pi r^2(1-\cos\theta)h_{\text{i}}} \tag{3}$$

Here, θ is the contact angle of the droplet on the condensing surface. Due to the effect of the vapor–liquid interfacial curvature, the temperature difference can be expressed as [26]

$$\Delta T_{\text{c}} = \frac{2T_{\text{s}}\sigma_{\text{lv}}}{H_{\text{fg}}\rho r} \tag{4}$$

In most previous studies [12,24,28–30], the assumption adopted in their models was made that the droplet is small enough, so the conduction is the primary mechanism during heat transfer through droplets of all sizes. The assumption is feasible if it is for the dropwise condensation on the plate wall in which the shape and position of all sized droplets are independent of each other and almost have no change. Due to the changing inclination angle of droplets on the circumference along the horizontal tube, the convection effect inside the droplet should be taken into consideration. Based on the expression proposed by Fatica and Katz [27] for the plate wall, we introduced the inclination angle into the shape factor function $f(\theta, \alpha)$ to consider both the convection effect and condensation on horizontal tube surface, and thus the temperature difference owing to the thermal resistance through the droplet can be revised as

$$\Delta T_{\text{d}} = \frac{\Phi}{2\pi r\lambda\sin\theta f(\theta,\alpha)} \tag{5}$$

Here, the shape factor is just a function respect to the contact angle and inclination angle and it is independent of subcooling, thermal properties and other parameters. To obtain the shape factor, using numerical simulation with CFD package Ansys 14.0, we firstly acquire the heat rate Φ resulting from a certain temperature difference ΔT_{d} between the top and bottom surfaces of the single droplet by considering the convection effect. Results of the shape factor function obtained by the present method are shown in Fig. 2. To compare with the equivalent cylinder method [28] and the method of integration of temperature difference between two neighboring isothermal surfaces [29] without considering the convection effect, we also compute the shape factor in the present numerical method based on the pure conduction. It can be seen that the shape factor function calculated by the present numerical method intermediates between the two compared models of [28] and [29], when the contact angle is larger than 90°. And the deviation among these three methods is resulted from the different simplifications during the calculations. As shown in Fig. 2, when the droplet locates at various positions along the circumference of horizontal tube, i.e. at the inclination angle of 0°, 90°, and 180°, all the results by the present numerical method considering the convection effect inside the droplet are larger than those without considering the convection effect. Because the convection effect can strengthen the disturbance inside the condensing droplets. Fig. 3 displays the shape factor function $f(\theta, \alpha)$ respect to the inclination angle at contact angle of 90°, 120° and 150°. We can find that the contact angle has a great influence on the shape factor function, as well as the inclination angle α. The large contact angle can produce small heat transfer resistance through the single droplet itself. In addition, when the inclination angle is about 90°, the convection effect inside the droplet achieves the largest so the heat transfer resistance of the droplet at this location is the lowest and it corresponds to the largest shape factor. Through above analysis, the convection effect inside the droplets should be introduced to the theoretical prediction of the dropwise condensation, especially for the condensation on horizontal tube.

As mentioned in Section 2.1, the temperature difference caused by the effect of the coating layer adhering to the condensing surface can be given by

$$\Delta T_{\text{coat}} = \frac{\delta_{\text{coat}}\Phi}{\lambda_{\text{coat}}\pi(r\sin\theta)^2} \tag{6}$$

Owing to the subcooling of the condensing surface, the minimum viable droplet radius can be written as [25,29,30]

$$r_{\text{min}} = \frac{2T_{\text{s}}\sigma_{\text{lv}}}{H_{\text{fg}}\rho\Delta T} = \frac{\Delta T_{\text{c}}}{\Delta T}r \tag{7}$$

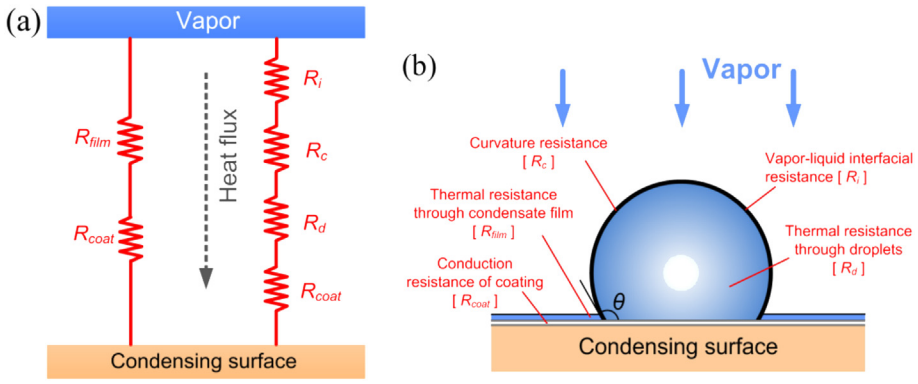

Fig. 1. Schematic of heat transfer resistance in dropwise condensation.

The total temperature difference through the single condensing droplet between the vapor and cool condensing surface is the sum of the above four temperature drops

$$\Delta T = \Delta T_i + \Delta T_c + \Delta T_d + \Delta T_{coat} \tag{8}$$

Therefore, based on the above theoretical analysis, Eqs. (3)–(8) can be combined to calculate the heat transfer rate through the single droplet in terms of radius r as

$$\Phi(r) = \frac{\Delta T - \Delta T_c}{\frac{1}{\pi r^2}\left(\frac{1+\cos\theta}{2h_i \sin^2\theta} + \frac{r}{2\lambda f(\theta,\alpha)\sin\theta} + \frac{\delta_{coat}}{\lambda_{coat}\sin^2\theta}\right)} \tag{9}$$

2.3. Drop-size distribution

During the complete process of dropwise condensation, a droplet may undergo growth, merger and departure on the condensing surface. Due to the randomness of nucleation sites, drop-size distribution must be obtained prior to establishing the overall dropwise condensation heat transfer model. And the stable dropwise condensation process can be achieved by the steady state drop-size distribution. For small droplets, they are assumed to grow up only by direct condensation of the vapor, and the drop-size distribution based on the population balance theory is presented in the literature [25,29–32]. We also employ this theory to model the dropwise condensation heat transfer. The steady state drop-size distribution is obtained based on the conservation of the number of droplets in a certain size range, i.e. the number of droplets entering a size range must be equal to the number of those leaving the same size range. The population density $n(r, \alpha)$ for small droplets growing up by direct condensation is defined as the number of droplets of radius r on the condensing surface with tilted angle α per unit area. It can be written as [29]

$$n(r,\alpha) = \frac{r}{3\pi r_e^3 r_{max}(\alpha)}\left(\frac{r_e}{r_{max}(\alpha)}\right)^{-\frac{2}{3}} \frac{r_e - r_{min}}{r - r_{min}} \frac{A_2 r + A_3}{A_2 r_e + A_3} \exp(B_1 + B_2) \tag{10}$$

where parameters such as B_1, B_2 and so on can be referred in Ref. [29]. For large droplets, the drop-size distribution $N(r, \alpha)$ on the tilted surface should satisfy [30,33]

$$N(r,\alpha) = \frac{1}{3\pi r^2 r_{max}(\alpha)}\left(\frac{r}{r_{max}(\alpha)}\right)^{-\frac{2}{3}} \tag{11}$$

where r_{max} is the size of departure droplet, i.e., the maximum droplet radius. Note that in the present calculation, the inclination angle α is introduced into r_{max} of Eqs. (10) and (11), which can determine the population density at different positions. The maximum droplet radius r_{max} on the condensing surface of a horizontal tube is not fixed at different locations along the circumferential direction, which can be simplified as the size of a departure droplet on the surface with different inclination angles. If there is

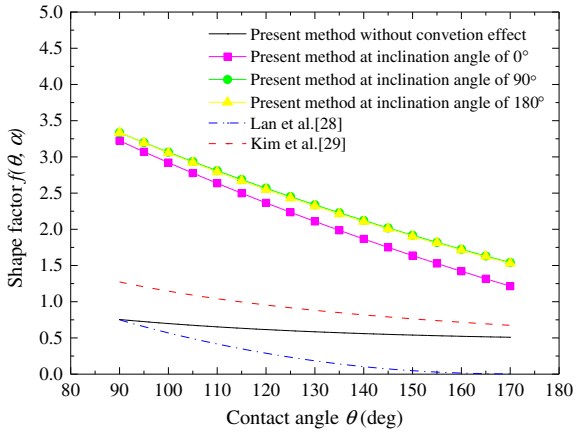

Fig. 2. Relation between contact angle and shape factor.

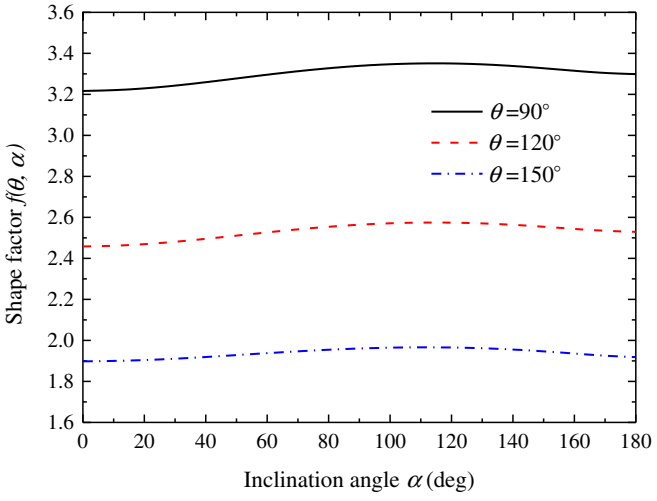

Fig. 3. Relation between inclination angle and shape factor.

no other external force, the size of the departure droplet can be established by the force balance of surface tension force between the condensing surface and droplet and the gravity force schematic in Fig. 4(a). Then, since the contact angle is assumed to be fixed, the gravity force on the droplet shedding from the condensing surface with inclination angle α can be expressed as

$$F_g = \frac{2-3\cos\theta+\cos^3\theta}{3}\pi r^3\rho g\sin\alpha \tag{12}$$

As shown in Fig. 4(b) from the top view, the outline of the condensing surface wetted by the droplet is assumed as an ideal circle, and then the overall surface tension on the droplet is obtained by integration with respect to the angle β

$$dF_c = \sigma\cos\theta'\cos\beta ds \tag{13}$$

$$F_c = 2\int_0^{\pi}\sigma\cos\theta'\cos\beta ds \tag{14}$$

In Eq. (14), the local solid–liquid contact angle θ' increases from the receding contact angle θ_r to the advancing contact angle θ_a along the wetted surface outline. Cornwell et al. [34,35] proposed a relationship between the local contact angle θ' and the angle β as

$$\cos\theta' = \left(\frac{\cos\theta_a+\cos\theta_r}{2}\right)+\left(\frac{\cos\theta_r-\cos\theta_a}{2}\right)\cos\beta \tag{15}$$

The arc length ds can be written as

$$ds = \frac{1}{2}d_c d\beta \tag{16}$$

Substituting Eq. (15) and Eq. (16) into Eq. (14) produces the surface tension force as a function of the angle β

$$F_c = \sigma d_c\int_0^{\pi}\left[\left(\frac{\cos\theta_a+\cos\theta_r}{2}\right)\cos\beta + \left(\frac{\cos\theta_r-\cos\theta_a}{2}\right)\cos^2\beta\right]d\beta \tag{17}$$

Further, it can be written as

$$F_c = -\frac{\pi}{2}\sigma r\sin\theta(\cos\theta_a-\cos\theta_r) \tag{18}$$

where the value of $(\cos\theta_a-\cos\theta_r)$ increases with the increasing inclination angle α. Based on the force balance between Eqs. (12) and (18), the radius of departure drop can be finally deduced as

$$r_{max}(\alpha) = \left[\frac{3\sigma\sin\theta(\cos\theta_r-\cos\theta_a)}{2\rho g\sin\alpha(2-3\cos\theta+\cos^3\theta)}\right]^{1/2} \tag{19}$$

2.4. Dropwise condensation heat transfer on a horizontal tube

The contact area between droplets of all sizes and the condensing surface can be calculated with integration to the population density of droplets. The integration region of the equations is within the range of 1/2 of the circle due to the symmetry of the geometry. Thus, in terms of a fixed contact angle, the contact area ϕ_1 between small droplets and condensing surface, and contact area ϕ_2 between large droplets and condensing surface can be expressed as follows.

$$\phi_1 = \int_0^{\pi}\int_{r_{min}}^{r_e}\pi(r\sin\theta)^2 n(r,\alpha)drd\alpha \tag{20}$$

$$\phi_2 = \int_0^{\pi}\int_{r_e}^{r_{max}}\pi(r\sin\theta)^2 N(r,\alpha)drd\alpha \tag{21}$$

The ratio of the non-occupied area of condensing droplets to the occupied area is defined as

$$\eta = \frac{A_e}{\phi_1+\phi_2} \tag{22}$$

Here, A_e is the bare area on the condensing surface of the horizontal tube, i.e. the non-occupied area of condensing droplets.

To simplify the calculation, we assume that the condensing surface of a horizontal tube is composed of numerous inclined plates with different inclination angles as shown in Fig. 4(c) and the length is infinite in the axial direction. Therefore, the heat flux during dropwise condensation on the horizontal tube is obtained by adding the ones through droplets of all sizes and through the adsorbed condensate film.

$$q = \frac{1}{1+\eta}\left[\int_0^{\pi}\int_{r_{min}}^{r_e} n(r,\alpha)\Phi(r)drd\alpha + \int_0^{\pi}\int_{r_e}^{r_{max}(\alpha)} N(r,\alpha)\Phi(r)drd\alpha\right] + \frac{\eta}{1+\eta}h_{film}\Delta T \tag{23}$$

Note that by neglecting the impact of gravity on the thickness of adsorbed condensate film, the interval of the above integral formula is from 0 to π owing to the symmetric geometry of the horizontal tube. Finally, the average heat transfer coefficient in the stable dropwise condensation process can be calculated as

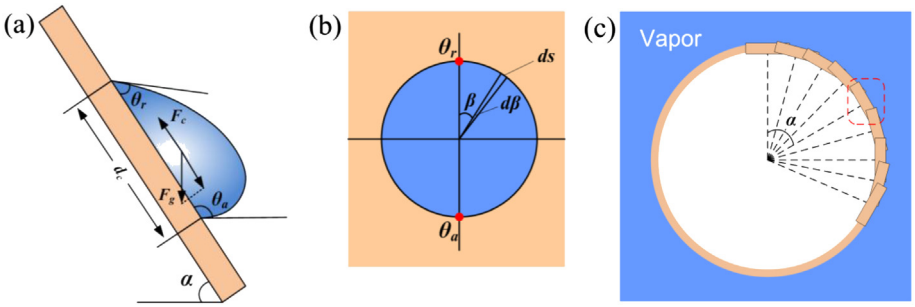

Fig. 4. Schematic of droplet force on inclined surface and simplified geometric structure of horizontal tube.

$$h_{av} = \frac{q}{\Delta T} \tag{24}$$

3. Results and discussion

3.1. Heat transfer performance for a single droplet

According to the analysis of the previous section, we can find that both the temperature drop due to the vapor–liquid interfacial resistance and heat transfer resistance through the single droplet itself are related to the contact angle. Fig. 5 shows the total heat transfer resistance against contact angle and droplet radius. It can be seen that the heat transfer resistance for the individual droplet increases with the increasing contact angle. The heat transfer rate and heat flux through the single droplet with different contact angles, droplet sizes and subcoolings at the vapor pressure of 0.1 MPa are also presented in Figs. 6 and 7, respectively. The heat transfer rate of the single droplet with a fixed radius decreases as its contact angle increases, but the bottom area of the droplet decreases even more greatly. Since all the heat transfers through the bottom of the droplet, the heat flux behaves in the opposite trend. As can be concluded, for the single droplet, a larger contact angle and smaller droplet radius can result in higher heat transfer resistance.

3.2. Dropwise condensation heat transfer performance

The present model using the result of Eq. (23) predicts the heat flux on the horizontal tube with different contact angles, subcoolings and condensate film thicknesses at an atmospheric pressure in Fig. 8. It is seen that the effect of the contact angle on the heat transfer during the dropwise condensation process is significant. Both a great contact angle and a large subcooling can produce a high heat flux. Although a larger contact angle can cause a higher thermal resistance for the single droplet, the droplet is more unstable and falling off more easily, and the disturbance caused by the dropwise condensation is enhanced, and thus the heat transfer can be increased in the whole process. Similarly, the thickness of adsorption condensate film has a remarkable impact on the heat flux. A thin adsorbed condensate film is preferred due to the minimal thermal resistance.

Fig. 9 displays the average heat transfer coefficient for various liquid–solid interfacial interactions in terms of the subcooling temperature and contact angle. The computation is carried out under the conditions of contact angles of 90°, 120° and 150°, the condensate film thickness of 5 μm, and the condensing pressure of 0.1 MPa. From Fig. 9, it can be seen that the average heat transfer coefficient reduces as the subcooling increases. Due to the increased condensate on the tube surface, the additional heat conduction resistance from the vapor to condensing surface of the tube increases. And the mechanism of enhanced heat transfer is the same as the above: a larger contact angle results in a higher heat transfer coefficient of dropwise condensation.

The results of dropwise condensation heat flux against subcooling at various pressures are shown in Fig. 10 for contact angle of 120° and thickness of adsorbed condensing film of 5 μm. It can be observed that the heat flux increases with the increase of the operating pressure at the same subcooling. Because a high pressure of vapor can produce a low vapor–liquid interfacial resistance, and the number of droplets formed in the dropwise condensation process also increases. In addition, the increase of vapor saturation temperature can result in the decrease of the surface tension of the condensate. As the vapor pressure increases, the droplets can easily fall off from the surface and the increasing heat flux of dropwise condensation is achieved.

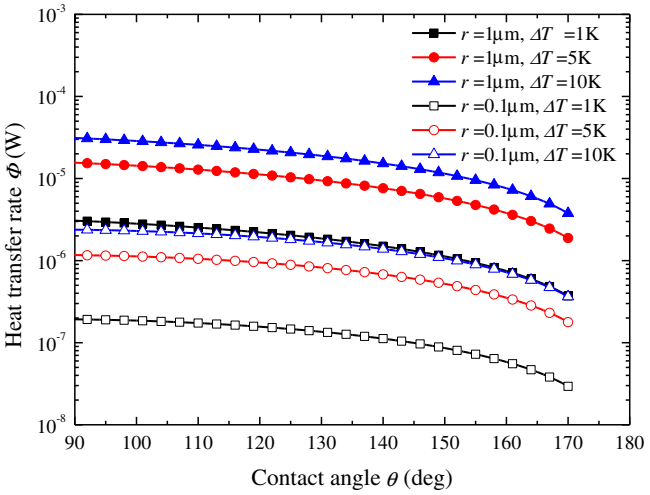

Fig. 6. Heat transfer rate against contact angle at various radiuses of a single droplet.

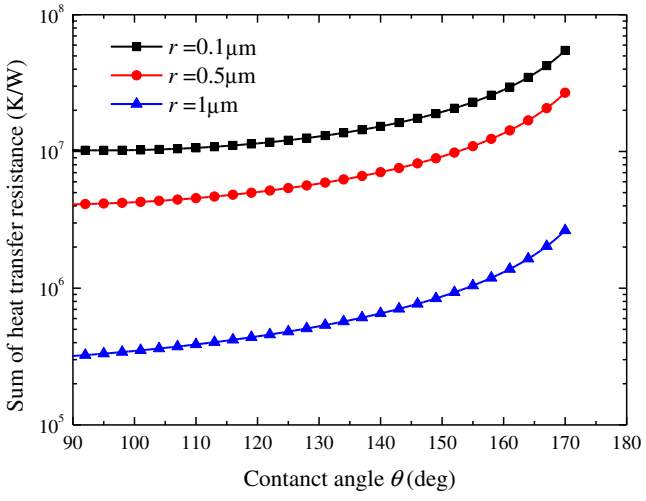

Fig. 5. Total thermal resistance against contact angle at various radiuses of a single droplet.

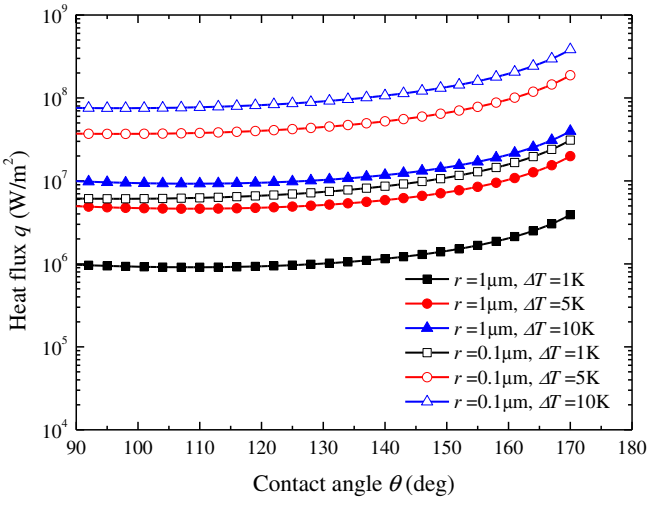

Fig. 7. Heat flux against contact angle at various radiuses of a single droplet.

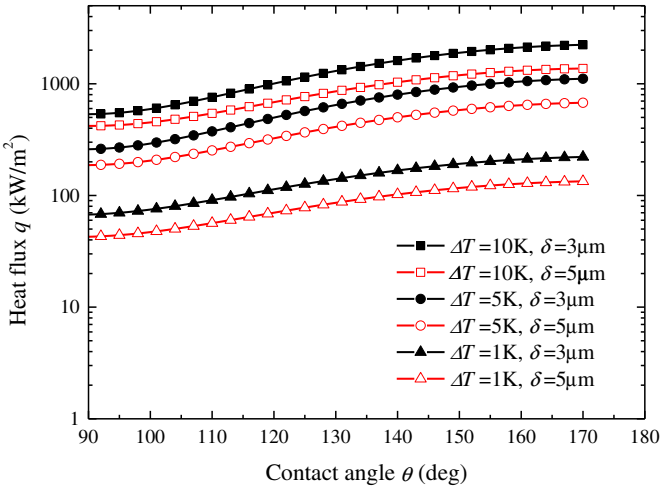

Fig. 8. Dropwise condensation heat flux respect to contact angle, subcooling and condensate film thickness.

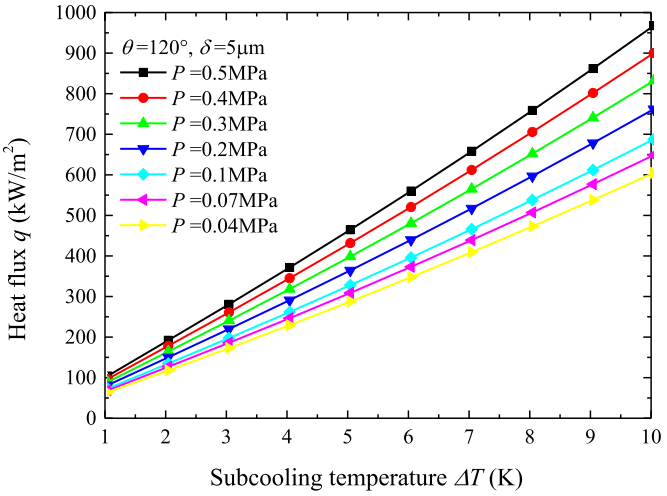

Fig. 10. Dropwise condensation heat flux against subcooling at various pressures.

3.3. Comparison with Nusselt theoretical and experimental data

In Fig. 11, the comparison with film condensation of Nusselt theory verifies that the dropwise condensation is a superior heat transfer mode to film condensation. The heat flux of dropwise condensation increases with the contact angle at the same subcooling temperature. At the subcooling of 5 K and the vapor pressure of 0.1 MPa, the heat flux increases by 147% at contact angle of 90° and by 669% at contact angle of 150° compared with that of film condensation. In previous theoretical and experimental studies reported by Refs. [15,29,36,37], the dropwise condensation heat transfer performance is approximately enhanced by 1.3–5.5 times compared with film condensation of Nusselt theory.

In addition, the present model predicts the average heat transfer coefficient in comparison with available experimental data [36] in Fig. 12(a). The stable dropwise condensation on stainless steel tubes by plasma-ion implantation was experimentally achieved, and the experimental data 1 and 2 were obtained in the conditions of ion doses of 10^{16} and 10^{15} N/cm^2, respectively [36]. The calculation is based on the conditions of the contact angle of 90° and the condensate film thickness of 5 μm since the contact angle in the experiment is unavailable. From Fig. 12(a), the predicted and experimental data are in good agreement within a low subcooling range, however, the deviation increases with the increase of the subcooling. The maximum relative error of the average heat transfer coefficient is within 34.8%, which is partly due to both the simplification in the present model and measurement uncertainties in the experiment. The assumption (5) in Section 2 neglects the non-uniform distribution of droplets outside the horizontal tube surface, so the heat flux calculated by the present model deviates to higher side, especially for large subcooling temperature.

Fig. 12(b) shows the comparison of heat flux between the present model and experimental data in Ref. [37]. The copper alloy tube using self-assembled monolayers with the measured contact angles of 111.2° and 148.5° was experimentally studied in steady-state at a constant pressure of 33.86 kPa. As shown in Fig. 12(b), the results by the present model and the experimental data are in better agreement in a low subcooling range, while the difference increases gradually with the increasing subcooling. On one hand, in the experiment, the large subcooling temperature could produce more condensate. Thus, instead of the perfect dropwise condensation, the film condensation could appear on the surface, especially on the bottom of the horizontal tube, which caused a smaller experimental heat flux. On the other hand, Tsuruta and Tanaka

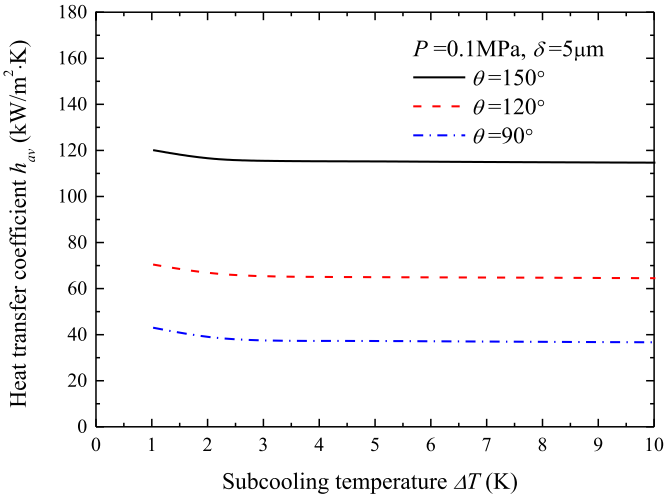

Fig. 9. Average heat transfer coefficient respect to contact angle and subcooling.

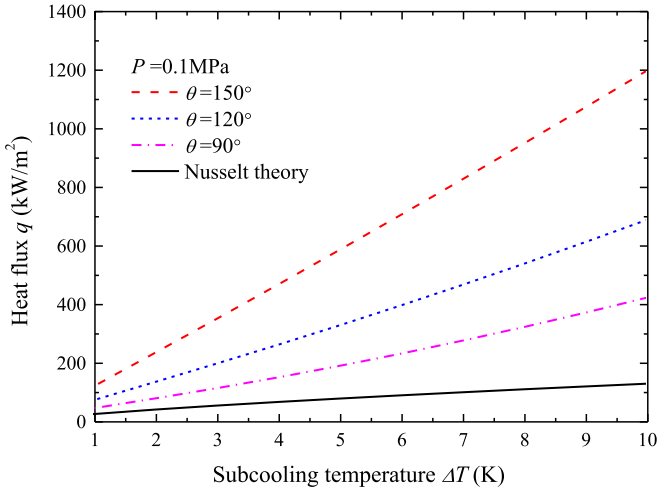

Fig. 11. Comparison between the present model prediction and Nusselt theory.

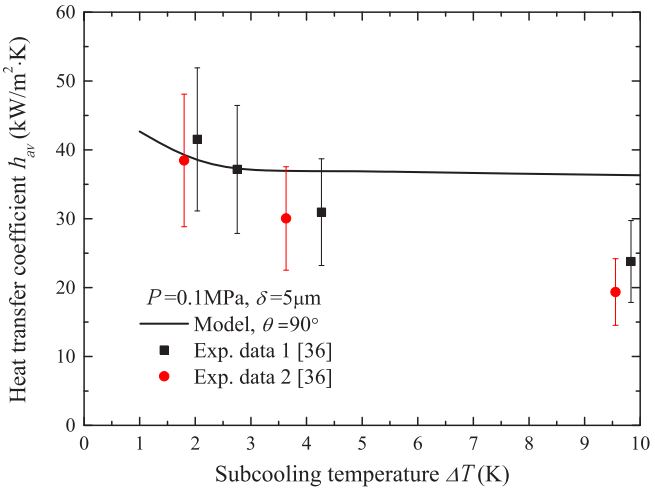

Fig. 12. Comparison between the present model prediction and available experimental data.

[38,39] mentioned that constriction resistance on the condensing surface had a large effect on the heat transfer at low pressure. During the calculation at the pressure of 33.86 kPa, we ignored the influence of constriction resistance on heat transfer as mentioned in the assumption (6) in Section 2. And from Fig. 12(b), it is also seen that the deviation between the present model and experimental data is larger at the contact angle of 148.5° compared to the contact angle of 111.2°. The droplet at a higher contact angle is more unstable and falling off from top to bottom on the horizontal tube surface more easily, thus the excessive condensate could accumulate at the bottom for a short time in the experiment, which adds an extra thermal resistance. This probably causes the heat transfer performance of experiment data to a lower side, especially at high contact angles. Therefore, the present model is more suitable to predict dropwise condensation heat transfer on the horizontal tube for not large subcooling and contact angle.

4. Conclusions

The characteristics of stable dropwise condensation heat transfer on the horizontal tube have been investigated theoretically. The conclusions are drawn as follows:

(1) The stable dropwise condensation heat transfer model based on the droplets and film coexisting condensation mechanism on the horizontal tube has been established. Through the analysis of all the contributing thermal resistances, the convection effect inside droplets themselves has also been taken into consideration in the present model, which can compute the overall heat flux by dropwise condensation on horizontal tube.

(2) For the single droplet, both the temperature drop due to the vapor–liquid interfacial resistance and the heat transfer resistance through the single droplet itself are related to the contact angle. It is shown that the large contact angle and small droplet radius can produce high heat transfer resistance.

(3) The contact angle and adsorbed condensate film thickness between droplets have been introduced into the present model by incorporating with drop-size distribution on the horizontal tube and their influences on the dropwise condensation process have also been discussed. It can be found that a large contact angle, a high vapor pressure and a thin adsorbed condensate film can result in a high heat flux and a great average heat transfer coefficient. The present theoretical model is also validated by comparing with available experimental data and it shows that the present model can successfully predict dropwise condensation heat transfer on the horizontal tube within not large subcooling and contact angle range.

Acknowledgements

This work is supported by the National Natural Science Foundation of China (No. 51222604) and the National Basic Research Program of China (973 Program) (No. 2011CB710702).

References

[1] W. Nusselt, Die Oberfalchencondensation des Wasserdampfes, Z. Ver. Dt. Ing. 60 (1916) 541–569.
[2] H.S. Wang, H. Honda, S. Nozu, Modified theoretical models of film condensation in horizontal microfin tubes, Int. J. Heat Mass Transfer 45 (7) (2002) 1513–1523.
[3] H.S. Wang, J.W. Rose, H. Honda, A theoretical model of film condensation in square section horizontal microchannels, Chem. Eng. Res. Des. 82 (4) (2004) 430–434.
[4] H.S. Wang, J.W. Rose, Film condensation in horizontal circular section microchannels, Int. J. Eng. Syst. Model. Simulat. 1 (2) (2009) 115–121.
[5] Q. Su, G.X. Yu, H.S. Wang, J.W. Rose, Microchannel condensation: correlations and theory, Int. J. Refrig. 32 (6) (2009) 1149–1152.
[6] M. Jakob, Heat transfer in evaporation and condensation, Mech. Eng. 58 (1936) 729–739.
[7] E. Ruckenstien, H. Metiu, On dropwise condensation on a solid surface, Chem. Eng. Sci. 20 (3) (1965) 173–180.
[8] G. Tammann, W. Boehme, Die Zahl der Wassertröpfchen bei der Kondensation auf verschiedenen festen Stoffen, Ann. Physik 414 (1) (1935) 77–80.
[9] A. Umur, P. Griffith, Mechanism of dropwise condensation, ASME J. Heat Transfer 87 (2) (1965) 275–282.
[10] C. Yamali, H. Merte, A theory of dropwise condensation at large subcooling including the effect of the sweeping, Heat Mass Transfer 38 (3) (2002) 191–202.
[11] C.F. Mu, J.J. Pang, Q.Y. Lu, T.Q. Liu, Effect of surface topography of material on dropwise condensation nucleation site density, Chem. Eng. Sci. 63 (4) (2008) 874–880.
[12] Y.J. Song, D.Q. Xu, J.F. Lin, A study on the mechanism of dropwise condensation, Int. J. Heat Mass Transfer 34 (11) (1991) 2827–2831.
[13] A. Majumdar, I. Mezic, Instability of ultra-thin water films and the mechanism of droplet formation on hydrophilic surfaces, ASME J. Heat Transfer 121 (4) (1999) 964–971.
[14] T. Haraguchi, K. Yoshimia, H. Kato, Determination of density and vacancy concentration in rapidly solidified FeAl ribbons, Intermetallics 11 (7) (2003) 707–711.
[15] M.H. Rausch, A. Leipertz, A.P. Froba, Dropwise condensation of steam on ion implanted titanium surfaces, Int. J. Heat Mass Transfer 53 (1–3) (2010) 423–430.

[16] R.J.E. Walpot, F.L.A. Ganzevles, C.W.M. Van der Geld, Effects of contact angle on condensate topology, drainage and efficiency of a condenser with mini-channels, Exp. Therm. Fluid Sci. 31 (8) (2007) 1033–1042.
[17] G.D. Bansal, S. Khandekar, K. Muralidhar, Measurement of heat transfer during drop-wise condensation of water on polyethylene, Nanoscale Microscale Thermophys. Eng. 13 (3) (2009) 184–201.
[18] A.K. Das, H.P. Kilty, P.J. Marto, G.B. Andeen, A. Kumar, The use of an organic self-assembled monolayer coating to promote dropwise condensation of steam on horizontal tubes, ASME J. Heat Transfer 122 (2) (2000) 278–286.
[19] X.H. Ma, J.B. Chen, D.Q. Xu, J.F. Lin, C.S. Ren, Z.H. Long, Influence of processing conditions of polymer film on dropwise condensation heat transfer, Int. J. Heat Mass Transfer 45 (12) (2002) 3405–3411.
[20] G.X. Pang, J.D. Dale, D.Y. Kwok, An integrated study of dropwise condensation heat transfer on self-assembled organic surfaces through Fourier transform infra-red spectroscopy and ellipsometry, Int. J. Heat Mass Transfer 48 (2) (2005) 307–316.
[21] B.M. Yu, P. Cheng, Fractal models for the effective thermal conductivity of bidispersed porous media, J. Thermophys. Heat Transfer 16 (1) (2002) 22–29.
[22] Y.T. Wu, C.X. Yang, X.G. Yuan, Drop distribution and numerical simulation of dropwise condensation heat transfer, Int. J. Heat Mass Transfer 44 (23) (2001) 4455–4464.
[23] F.Z. Sun, M. Gao, S.H. Lei, Y.B. Zhao, K. Wang, Y.T. Shi, N.H. Wang, The fractal dimension of the fractal model of dropwise condensation and its experimental study, Int. J. Nonlinear Sci Numer. Simul. 8 (2) (2007) 211–222.
[24] M.F. Mei, B.M. Yu, J.C. Cai, L. Luo, A fractal analysis of dropwise condensation heat transfer, Int. J. Heat Mass Transfer 52 (21–22) (2009) 4823–4828.
[25] M. Abu-Orabi, Modeling of heat transfer in dropwise condensation, Int. J. Heat Mass Transfer 41 (1) (1998) 81–87.
[26] J.W. Rose, Dropwise condensation theory, Int. J. Heat Mass Transfer 24 (2) (1981) 191–194.
[27] N. Fatica, D.L. Katz, Dropwise condensation, Chem. Eng. Prog. 45 (11) (1949) 661–674.
[28] Z. Lan, X.H. Ma, X.D. Zhou, M.Z. Wang, Theoretical study of dropwise condensation heat transfer: effect of the liquid-solid surface free energy difference, J. Enhanced Heat Transfer 16 (1) (2009) 61–71.
[29] S. Kim, K.J. Kim, Dropwise condensation modeling suitable for superhydrophobic surfaces, ASME J. Heat Transfer 133 (8) (2011) 081502.
[30] S. Vemuri, K.J. Kim, An experimental and theoretical study on the concept of dropwise condensation, Int. J. Heat Mass Transfer 49 (3–4) (2006) 649–657.
[31] H. Tanaka, A theoretical study of dropwise condensation, ASME J. Heat Transfer 97 (1) (1975) 72–98.
[32] J.R. Maa, Drop size distribution and heat flux of dropwise condensation, Chem. Eng. J. 16 (3) (1978) 171–176.
[33] E.J. Le Fevre, J.W. Rose, A theory of heat transfer by dropwise condensation, in: Proceedings of the 3rd International Heat Transfer Conference, vol. 2, 1966, pp. 362–375.
[34] K. Cornwell, R.B. Schuller, A study of boiling outside a tube bundle using high speed photography, Int. J. Heat Mass Transfer 25 (5) (1982) 683–690.
[35] K. Cornwell, The influence of bubbly flow on boiling from a tube in a bundle, Int. J. Heat Mass Transfer 33 (12) (1990) 2579–2584.
[36] A. Bani Kananeh, M.H. Rausch, A.P. Froba, A. Leipertz, Experimental study of dropwise condensation on plasma-ion implanted stainless steel tubes, Int. J. Heat Mass Transfer 49 (25–26) (2006) 5018–5026.
[37] S. Vemuri, K.J. Kim, B.D. Wood, S. Govindaraju, T.W. Bell, Long term testing for dropwise condensation using self-assembled monolayer coatings of *n*-octadecyl mercaptan, Appl. Therm. Eng. 26 (4) (2006) 421–429.
[38] T. Tsuruta, H. Tanaka, A theoretical study on the constriction resistance in dropwise condensation, Int. J. Heat Mass Transfer 34 (11) (1991) 2779–2786.
[39] T. Tsuruta, H. Tanaka, Experimental verification of constriction resistance theory in dropwise condensation heat transfer, Int. J. Heat Mass Transfer 34 (11) (1991) 2787–2796.